MPMI Vol. 20, No. 7, 2007, pp. 857–866. doi:10.1094/MPMI-20-7-0857.

e-Xtra*

Protein Accumulation in the Germinating *Uromyces appendiculatus* Uredospore

Bret Cooper,[1] Anil Neelam,[1] Kimberly B. Campbell,[1] Joohyun Lee,[1] George Liu,[2] Wesley M. Garrett,[3] Brian Scheffler,[4] and Mark L. Tucker[1]

[1]Soybean Genomics and Improvement Laboratory, 10300 Baltimore Ave., Bldg. 006 Rm 213, United States Department of Agriculture–Agricultural Research Service (USDA-ARS), Beltsville, MD 20705, U.S.A.; [2]Bovine Functional Genomics Lab, and [3]Biotechnology and Germplasm Laboratory, 10300 Baltimore Ave., Bldg. 200, USDA-ARS, Beltsville, MD 20705, U.S.A.; [4]MSA Genomics Laboratory, 141 Experiment Station Road, USDA-ARS, Stoneville, MS 38776, U.S.A.

Submitted 4 January 2007. Accepted 2 March 2007.

***Uromyces appendiculatus* is a rust fungus that causes disease on beans. To understand more about the biology of *U. appendiculatus*, we have used multidimensional protein identification technology to survey proteins in germinating asexual uredospores and have compared this data with proteins discovered in an inactive spore. The relative concentrations of proteins were estimated by counting the numbers of tandem mass spectra assigned to peptides for each detected protein. After germination, there were few changes in amounts of accumulated proteins involved in glycolysis, acetyl Co-A metabolism, citric acid cycle, ATP-coupled proton transport, or gluconeogenesis. Moreover, the total amount of translation elongation factors remained high, supporting a prior model that suggests that germlings acquire protein translation machinery from uredospores. However, germlings contained a higher amount of proteins involved in mitochondrial ADP:ATP translocation, which is indicative of increased energy production. Also, there were more accumulating histone proteins, pointing to the reorganization of the nuclei that occurs after germination prior to appressorium formation. Generally, these changes are indicative of metabolic transition from dormancy to germination and are supported by cytological and developmental models of germling growth.**

Additional keywords: mass spectrometry, proteomics.

Dry edible bean crops rank among the top 10 cash-producing vegetables in the United States, and U.S. farmers rank sixth in the world in terms of production (Lucier and Jerardo 2006). Although future infections of dry bean by *Phakopsora pachyrhizi* are imminent (Pastor-Corrales et al. 2006), *Uromyces* spp. are the most economically important fungi causing rust disease on *Phaseolus* spp. Reports of 13 to 54% yield losses to due to *Uromyces* spp. in North Dakota (Venette and Jones 1982) and 75% yield losses in irrigated commercial fields in Colorado (Schwartz 1984) have been the driving force behind continued biological research aimed at mitigating the rust lifecycle and understanding fungal interactions with susceptible or resistant bean plants.

Autoecious rusts such as *Uromyces* spp. can complete their asexual and sexual life stages on a single host. Although sexual teliospores can survive harsh overwintering conditions and lead to the next season's outbreak, growers and researchers are more often concerned with the asexual reproduction of the fungus because it occurs in rapid succession and results in the transmission of enormous amounts of windborne uredospores that quickly spread, and infect and destroy plants in neighboring fields, counties, and states.

When a uredospore lands on a susceptible leaf, if there are environmentally favorable conditions that include high humidity, droplets of water, and cool conditions (18 to 20°C) often found under the leaf canopy in the early morning, the spore germinates and the emerging germ tube grows across the leaf surface. The germ tube contains cytoplasm and two nuclei which migrate with the growing tip of the tube (Heath and Heath 1976). When the germ tube recognizes, through a thigmotropic response, the height differential between the leaf surface and a stomata, an appressorium forms at the tip of the germ tube (Hoch et al. 1987), at which point the cytoplasm and nuclei move into it. Then mitosis occurs, and a septum is formed to separate the swelling appressorium from the empty germ tube (Kwon and Hoch 1991). An infection peg forms from the appressorium and penetrates the stomata, at which point a substomatal vesicle develops and a second round of mitosis occurs (Heath and Heath 1976; Staples and Hoch 1988). Afterward, infection hyphae proliferate through the apoplastic space of the leaf. The formation of a haustorial mother cell and the haustoria, the cell structure that finally invaginates a leaf cell and uptakes nutrients from it (Voegele et al. 2001), results in parasitism. The journey from germination to haustoria formation can occur within hours (Mendgen et al. 2006). Once the fungus develops haustoria and acquires nutrients and energy from the host, it forms uredia, the asexual reproductive bodies that rupture through the leaf epidermis and release more uredospores into the environment. Disease is a combination of parasitism and leaf damage, and the color of uredospores sloughing off the leaf is the namesake of the disease.

It is presumed that the fungus does not obtain nutrients from the host until haustoria form; therefore, it follows that the uredospore contains all of the necessary resources and energy reserves to complete its eventful journey. In a previous exami-

Corresponding author: B. Cooper; Telephone: +1 301-504-9892; Fax: +1 301-504-5728; E-mail: bret.cooper@ars.usda.gov

Nucleotide sequence data are available at GenBank dbEST under accession numbers EH294895 to EH306219.

*The *e*-Xtra logo stands for "electronic extra" and indicates supplemental material is available online.

nation of proteins contained within uredospores, we detected a full complement of proteins required for protein production, including amino acid synthases, translation initiation and elongation factors, ribosomal proteins, tRNA synthases, post-translational modification enzymes, and protein degradation machinery (Cooper et al. 2006). We hypothesized that uredospores were prepared to produce proteins very rapidly upon germination without needing to expend limited energy resources assembling components de novo. Coinciding with this evidence was our finding of a large number of heat-shock-related proteins within the uredospores. We postulated that the heat-shock-related proteins were cooperating with translation elongation factors and ribosomal proteins to maintain the integrity of the folding confirmation of nascent polypeptides during translation (Beckmann et al. 1990; Frydman et al. 1994; Wegele et al. 2004) and proposed that the uredospore exists in a suspended translational state, ready for protein production upon germination but protected against dehydration required for dormancy (Cooper et al. 2006).

As part of our continuing investigation of the asexual life cycle of *Uromyces appendiculatus*, we have performed a proteomics study on the germinating uredospore. This stage reflects the emergence of fungal life from a dormant spore and should coincide with the accumulation of proteins important for the transition to a metabolically active state. The detection of proteins was specifically enhanced by the procurement of sequence information derived from the sequencing of *U. appendiculatus* cDNAs. To further evaluate the significance of these findings, we also have compared the germling data with that for the resting uredospore (Cooper et al. 2006), which enabled an evaluation of the relative amounts of proteins found in the uredospore and the germling.

RESULTS

Our general approach to identifying proteins from *U. appendiculatus* is nearly the same as we previously reported for identifying proteins from its uredospores (Cooper et al. 2006). Basically, proteins are extracted from the germlings (Fig. 1C) and digested with proteases, and the peptides are separated and analyzed by liquid chromatography–tandem mass spectrometry (Washburn et al. 2001). The tandem mass spectra then are compared with sequences in a protein database using Mascot software (Perkins et al. 1999), and corresponding peptide sequences are resolved. These peptide sequences are reassembled into a parsimonious set of proteins (Nesvizhskii and Aebersold 2005) whose functions can be deduced given the experimental conditions or resolved by comparison with other known proteins.

Since our last report, we have developed two bioinformatics resources that have greatly improved our ability to interpret our tandem mass spectral data, enhance protein detection, and provide for more meaningful discovery. The first is a Perl script, which allows us to obtain the best translation for an expressed sequence tag (EST) sequence based upon translated BLAST search information. The translated sequence then is added to the database that Mascot searches when inferring amino acid sequence information from tandem mass spectra. The second resource is PANORAMICS (Feng et al. 2007; Lee and Cooper 2006), which assembles a probability-based and parsimonious set of proteins from the peptides Mascot identifies. PANORAMICS probabilities, which are a measurement of the accuracy of the protein assemblies, are in line with false-positive rates that can be measured by performing reverse database searches. As a result, a more accurate dataset is produced compared with datasets produced from programs that are not probability-based (Yang et al. 2004).

The impetus for specifically extracting protein information from EST sequences was a byproduct of initial attempts at perfecting ways to assemble proteins from peptide sequences. Although Mascot will perform six-frame translations on a DNA sequence and then search the tandem mass spectra against all the possible peptide sequences from the six-frame translation, an assembled protein group can inadvertently contain peptide sequences derived from all forward and reverse reading frames. This is because many small candidate peptide sequences are produced from the incorrect reading frames. Given the five incorrect reading frames from which so many short peptide sequences can be generated and the increased size of the database that results from the additional sequences, the chance to make matches to the peptides from incorrect reading frames increases (Cargile et al. 2004). Consequently, if reading frame information is not specifically considered, protein groups can be assembled from peptides derived from incorrect reading frames. To circumvent this problem, we relied on an approach for identifying open reading frames found with a BLASTX search and then used that information to redirect the translation of the EST such that only the most likely protein sequence from one reading frame was used in the database. This process reduces false positive matches and incorrect assemblies derived from incorrect reading frames. As a result, our protein assemblies should be accurate with respect to the search database, given the fact that each record is associated with only one real or derived protein sequence. This is a considerable advance for performing proteomics on an organism such as *U. appendiculatus* whose genome has not been sequenced, but for which EST data is more readily obtainable.

To enhance our ability to identify *U. appendiculatus* proteins, we increased the amount of sequence information for *U. appendiculatus* by sequencing a cDNA library made from rust hyphae, haustoria, and uredia isolated from infected plants (Fig. 1A and B). Reverse-transcription polymerase chain reaction (RT-PCR) was used to asses the amount of residual plant RNA in the total amount of RNA extracted from the preparation, and several independent tests suggested that there was less than 5% plant RNA contamination (Fig. 2). We sequenced from both

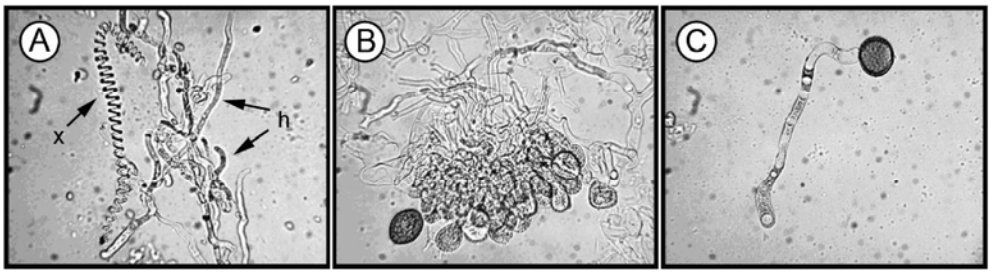

Fig. 1. Cell structures of *Uromyces appendiculatus*. **A,** Infection hyphae (h) and xylem (x) isolated from bean leaves 6 days postinoculation (dpi); **B,** uredia isolated from leaves 8 dpi; **C,** uredospore 4 h after induction for germination. Materials from samples represented in **A** and **B** were used for cDNA library construction while proteomic analysis was performed on germlings represented in **C.**

ends approximately 6,000 clones and generated 2,150 contigs and 238 singletons. Using an iterative BLAST search against known plant and fungal DNA and protein databases, we were able to identify 81 plant sequences, which composed 3.5% of the total and whose percentage was comparable with that predicted by RT-PCR. The plant sequences were removed from the file and the remaining 2,226 sequences were combined with *Uredinales* EST sequences culled from the National Center for Biotechnology Information (NCBI). Translated protein sequences based on BLASTX comparisons were derived using the Perl script, and 3,984 protein sequences from *U. appendiculatus*, other *Uromyces* spp., and related rusts such as *P. pachyrhizi* and *Puccinia graminis* were appended to a larger GenBank database of fungal protein sequences (Supplementary Data 1). This additional sequence information proved useful in identifying proteins unique to rusts that infect plants.

Thus, the final database that we used for Mascot searching included the translated EST sequences and all NCBI protein sequences classified in the kingdom Fungi. One complication of stitching together databases in this way is the compilation of redundant protein sequences. Fortunately, PANORAMICS efficiently handles redundant proteins in its parsimonious protein grouping strategy. One benefit from this grouping was that more insight on protein function could be gained by looking at the records of all proteins in the group. For example, one protein group with a probability of 0.9879 comprised four peptides that could be found in six protein records for *Neurospora crassa*, *Gibberella zeae*, *Chaetomium globosum*, and *Hypocrea jecorina*. All of these proteins are similar to 14-3-3-like proteins (Fig. 3). Two of the peptides were distinct, meaning that these peptides were associated only with these records. The two other peptides in the group also could be found among four and five other protein groups, meaning that these peptides were shared across several protein groups. The probability that the shared peptides belonged to any group was split when assessing the final group probability. However, it was the combination of distinct peptides and shared peptides that led to the high probability computed for this particular group. We interpret these results as suggesting that a protein from *U. appendiculatus* germlings is very similar to 14-3-3 proteins from these other organisms. In composing our table of identified proteins, we chose the *H. jecorina* record to represent the protein group because the descriptive information for this protein record provided the best insight to the possible function of the *U. appendiculatus* protein we had identified. Generally, the additional information gained by having multiple related proteins in our database helped us assign function to the assembled protein groups.

In our analysis of proteins extracted from germlings, we were able to detect 461 proteins at a 95% or better confidence level. Of these, 240 proteins were specific to sequences derived from the rust cDNA library, indicating the importance of the added protein sequence data. To simplify the analysis of the dataset, assembled protein groups were organized according to their Gene Ontology (GO) biological process. We identified germling proteins that are involved in glycolysis, acetyl Co-A metabolism, citric acid cycle, electron transport, ATP-coupled proton transport (ATPase subunit proteins), ADP:ATP translocation, and gluconeogenesis. In a broader context, these processes are part of a biological energy production pathway. Another set of proteins involved in processes such as amino acid metabolism, translation initiation and elongation, protein biosynthesis, protein folding, and proteolysis could be viewed as

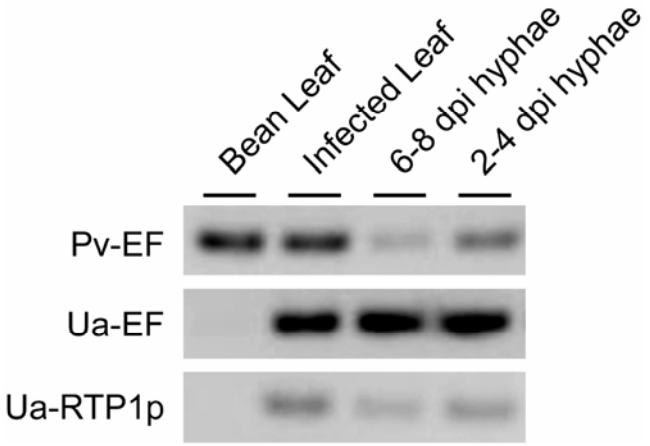

Fig. 2. Reverse-transcription polymerase chain reaction measurement of *Phaseolus vulgaris* α elongation factor (Pv-EF), *Uromyces appendiculatus* α elongation factor (Ua-EF) and *U. appendiculatus* RTP1p haustorium-specific protein (Ua-RTP1) mRNAs in noninfected *P. vulgaris* leaves, in *U. appendiculatus* infected *P. vulgaris* leaves, and in *U. appendiculatus* hyphal preparations from plants 2 to 4 and 6 to 8 days postinoculation (dpi).

Group probability: 0.9879

Peptide Sequence	Mascot Ion Score	Mascot Identity Score	Computed Peptide Mass	Observed Peptide Mass	Number of Spectra	Charge States	Peptide Class	Missed Cleavages	Peptide Probability
NLLSVAYK	38.75	47.1555	907.078	907.002	1	+2	shared(6)	0	0.3094
YLAEFASGEK	53.27	46.2976	1114.220	1113.792	2	+2	distinct	0	0.8177
DSTLIMQLLR	56.02	46.5320	1189.436	1189.262	7	+2	shared(5)	0	0.9326
YLAEFASGEKR	47.38	46.0950	1270.408	1270.282	6	+2 +3	distinct	1	0.8783

Protein Accession Number	Protein Mass	Protein Description
gi|85113192|ref|XP_964477.1|	30724.43	hypothetical protein ((AJ297911) 14-3-3-like protein [Hypocrea jecorina]) [Neurospora crassa OR74
gi|46108718|ref|XP_381417.1|	27636.84	hypothetical protein FG01241.1 [Gibberella zeae PH-1]
gi|88185868|gb|EAQ93336.1|	29924.35	hypothetical protein CHGG_01571 [Chaetomium globosum CBS 148.51]
gi|12054276|emb|CAC20378.1|	30594.12	14-3-3-like protein [Hypocrea jecorina]
gi|42545259|gb|EAA68102.1|	27636.84	hypothetical protein FG01241.1 [Gibberella zeae PH-1]
gi|28926261|gb|EAA35241.1|	30724.43	hypothetical protein ((AJ297911) 14-3-3-like protein [Hypocrea jecorina]) [Neurospora crassa]

Fig. 3. Example of a protein group assembled from peptides. Peptides are based on the match to *Uromyces appendiculatus* tandem mass spectra. Protein group probability, peptide sequences, Mascot Ions Scores and other data also are shown.

parts of protein metabolism pathways within the cell. A third set of proteins was viewed as having roles specific to the cell nucleus, such as those involved in nucleosome assembly (histones), gene transcription, nuclear protein translocation, and cell cycling. Other proteins, such as those involved in oxidation or reduction processes, were not as easily organized into supersets, whereas proteins such as actin, β-tubulin, and 14-3-3 proteins were easily organized but not as easily categorized because these proteins can be linked to multiple biological processes. There were 74 proteins with unknown or undefined functions and biological processes, and 5 of those proteins were derived from hypothetical translations of an EST.

To bring more meaning to our data, we compared the proteins discovered in germlings with the proteins previously described for the uredospore (Cooper et al. 2006). Given our assumption that uredospores contain proteins and resources to be used after germination, some of the same proteins found in uredospores also should be found in germlings, and we hypothesized that the detection of different amounts of these proteins could be explained by biological shifts from dormancy to cellular growth. Thus, to properly make the comparison, the uredospore tandem mass spectra were searched against our custom database, and proteins were assembled with PANORAMICS. This dataset contained 439 protein groups at a 95% confidence level, which is a reduction from the set of 468 proteins previously assembled with DBParser, a program that is not probability-based (Cooper et al. 2006; Yang et al. 2004). This data set is different from that described by Cooper and associates (2006) because of PANORAMICS and because of the additional *U. appendiculatus* data, to which 243 matches were made. As had been done for the germling proteins, the uredospore protein matches were organized based on GO Biological Process.

There are several reports whereby "spectral count," the number of times a tandem mass spectrum is recorded for a peptide, correlates linearly with the molar amount of a peptide in a sample (Liu et al. 2004). Consequently, the sum of spectral counts for peptides associated with a particular protein can be used to assess the amount of protein (Zybailov et al. 2005, 2006). Thus, we used the spectral count method to assess the relative amounts of 279 proteins that were common to the uredospore and germling datasets. An example is shown in Figure 4, where a protein matching a putative heat shock protein from *Cryptococcus neoformans* was found in uredospores and germ-

A Germling

Equivalent protein UAHYP_01B_F_H05_AB1_CONSENSUS match to heat shock protein sks2 mass 31472.81

Group probability: 1.0000

Peptide Sequence	Mascot Ion Score	Mascot Identity Score	Computed Peptide Mass	Observed Peptide Mass	Number of Spectra	Charge States	Peptide Class	Missed Cleavages	Peptide Probability
ANITITNSVGR	73.97	46.8871	1145.281	1145.362	2	2	distinct	0	0.9989
RANITITNSVG R	49.38	46.1893	1301.469	1301.112	5	2	distinct	1	0.9251
IQSLVSDFFGG R	57.04	45.9762	1325.487	1325.262	1	2	distinct	0	0.9817
SKVEDIVLVGG STR	75.85	45.6753	1459.663	1459.182	3	2	distinct	1	0.9949
				Total spectral count	11				

B Uredospore

Equivalent protein UAHYP_01B_F_H05_AB1_CONSENSUS match to heat shock protein sks2 mass 31472.81

Group probability: 1.000000

Peptide Sequence	Mascot Ion Score	Mascot Identity Score	Computed Peptide Mass	Observed Peptide Mass	Number of Spectra	Charge States	Peptide Class	Missed Cleavages	Peptide Probability
NTPIPTNK	43.41	46.0894	884	883.317	1	1	distinct	0	0.5644
RANITITNSVG R	66.76	46.0961	1301.469	1301.041	4	2	distinct	1	0.9967
IQSLVSDFFGG R	69.37	45.9707	1325.487	1325.547	17	3	distinct	0	0.9999
SKVEDIVLVGG STR	85.15	45.7082	1459.663	1459.597	3	3	distinct	1	0.9985
LEIEDSSADEL KK	42.1	45.8106	1476.601	1476.256	1	2	distinct	1	0.7507
LLGEFELSGIT PQPR	74.83	44.9944	1656.9	1656.447	80	2	distinct	0	0.9992
LSSAEIDQMIK DAESFK	48.68	44.4342	1912.142	1912.12	2	2	distinct	1	0.9478
				Total spectral count	108				

Fig. 4. Equivalent protein groups assembled from peptides for **A,** germlings and **B,** uredospores, with each group having a different number of peptides and spectra associated with those peptides. Peptides are based on the match to *Uromyces appendiculatus* tandem mass spectra. Protein group probability, peptide sequence, Mascot Ions Scores, other data also are shown.

lings. We summed the spectral count for all peptides for each protein and used the assumption that incongruence of having unequal protein coverage could be normalized (Zybailov et al. 2006). To do so, we adjusted each spectral count sum by dividing it by the mass of the protein and then dividing that by the sum of all adjusted spectral counts for all identified proteins in a dataset to create a normalized spectral abundance factor (NSAF) (Zybailov et al. 2006). By limiting the number of spectra used for spectral counts to only those spectra associated with an assembled protein (7,838 and 10,424 uredospore and germling spectra, respectively) rather than the total number of spectra collected by the mass spectrometer, we were able to determine the percentage of each protein in relation to all matched spectra. Subsequently, this enabled the measurement of relative differences in the concentration of detected proteins between germlings and uredospores. For example, using the protein resembling a heat shock protein from *C. neoformans*, there was 14.8 times more of this protein in the germling samples than in the uredospores (Fig. 4).

The relative abundance for all 279 proteins common to both uredospores and germlings was computed. Protein accumulation differences were discerned most easily when the proteins were organized by GO Biological Process and the summed NSAFs compared for each process (Fig. 5). When a strict five-fold change was used as a cut-off, the total amounts of detectable proteins involved in glycolysis, acetyl Co-A metabolism, citric acid cycle, ATP coupled proton transport, or gluconeogenesis remained relatively static. However, germlings contained a higher amount of proteins involved in mitochondrial transport (ADP:ATP translocation). At the protein metabolism level in germlings, there was a decrease in the amount of proteins involved in phosphate metabolism and ubiquitin-dependent protein catabolism. At the nuclear level in the germlings, more spectra were assigned to proteins involved in nucleosome assembly (histone proteins). However, the total levels of proteins involved in gene transcription (transcription factors) or proteins with roles in cell cycling fluctuated very little. As for other types of processes in germlings, there was a sharp increase in the detectable amounts of GTP-binding proteins with likely roles in vesicle trafficking.

An alternative view of the data reveals which specific proteins, rather than those grouped by GO Process, were most

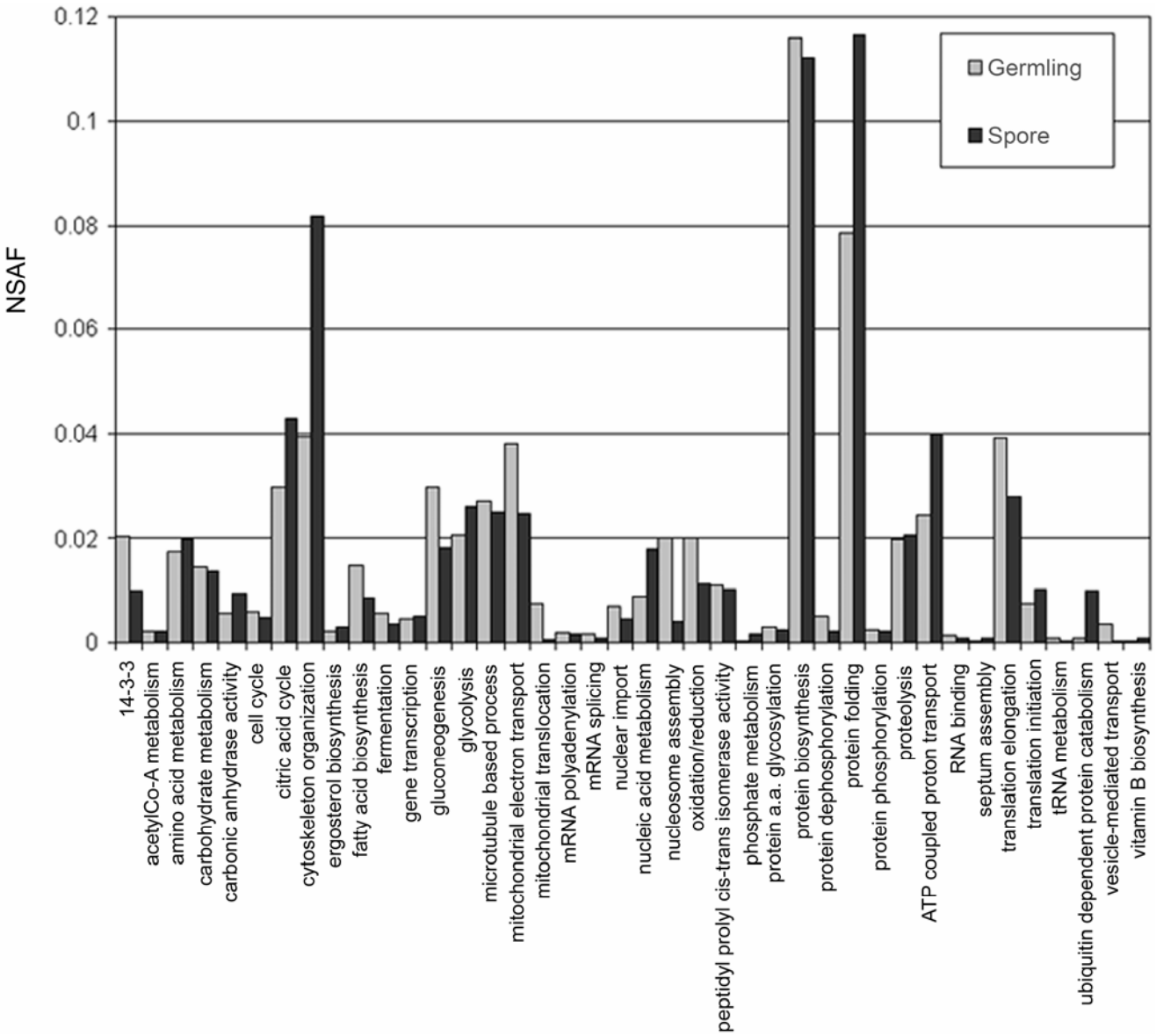

Fig. 5. Relative abundance of germling and uredospore proteins contributing to Gene Ontology Biological Process listed on the x-axis. Abundance is measured by the normalized spectral abundance factor (NSAF).

abundant. Although there appeared to be more glucose-6-phosphate isomerase in the germlings, there was more malate dehydrogenase in the uredospores. Likewise, there were several actin proteins in the uredospores that were not as readily detectable in the germlings. By contrast, the same could not be said for β-tubulin proteins that were equally abundant between the samples. The total amount of translation elongation factors also remained high and equally abundant, supporting a prior model that suggests that germlings acquire protein translation machinery from uredospores. A protein resembling septin was predominant in uredospores but not germlings. In addition, there were many proteins of unknown function that could be found in both the uredospores and germlings. Two proteins matching *U. appendiculatus* EST-derived protein sequences were predominant in germlings whereas six were predominant in uredospores.

When relaxing the cut-off for the NSAF fold-change to three, proteins in groups associated with ergosterol biosynthesis, fatty acid synthesis, oxidation or reduction, and vesicle-mediated transport appeared to be more abundant in the germlings. More chitinase appeared to accumulate in the germlings as well. From the other perspective, several more actin proteins and unknown proteins were more abundant in the uredospores.

Finally, there were many known and unknown proteins that were unique to the germling dataset but not the uredospore dataset, and vice versa. However, it is unknown whether these proteins are specific to germlings or uredospores, given the simple fact that random sampling effects associated with multidimensional protein identification technology dictate that not finding the protein is not proof that a protein is not in a sample (Liu et al. 2004). Further studies will be required to show if these are spore-specific or germling-specific proteins.

DISCUSSION

High-throughput liquid chromatography–tandem mass spectrometry has become a method of choice for detecting proteins in obligate pathogens and parasites that have been historically difficult to study (Florens et al. 2002; Hall et al. 2005; Smolka et al. 2003). Consequently, the proteomes of these organisms are being deciphered, and a greater understanding of their obligate nature and new ways of targeting the pathogens and parasites are emerging faster than ever before. As part of our ongoing interest in obligate plant pathogens, we are deciphering the proteomes of different life stages of *U. appendiculatus*, first with the resting uredospore (Cooper et al. 2006) and now the germinating uredospore.

The germling is just one of the many important life stages of *U. appendiculatus*, but is interesting primarily because it is one of the few life stages that can be easily studied in vitro and also is the emergent cell stage to make primary contact with the host plant. Successful infection depends on quick germling growth, followed by its formation of an appressorium and penetration of the interior of a leaf. We hypothesized that the spore contains all the necessary energy resources to allow the germling to perform this task and contains preassembled protein translation machinery, partially translated proteins, and many of the necessary proteins needed to become metabolically active. Our results suggest that there are very few major shifts in protein accumulation after germination, which supports our hypothesis. The shifts we have detected include an increase in ADP:ATP transporters, histones, peroxidase, acetyl-CoA acetyltransferases, and GTP-binding proteins. These changes may be indicative of increased energy production at the mitochondria, nuclear reorganization necessary for the first round of mitosis after appressorium formation, response to an increasingly oxidative environment, fatty acid synthesis that could be required for germ tube elongation, and increased vesicle trafficking. Generally, the observed increases fit well with a model whereby there is a shift from dormancy to a metabolically active state.

Our results agree with biochemical models for energy production. Malate deyhydrogenase, which is abundant in uredospores, completes the citric acid cycle by converting malate to oxaloacetate. Because uredospores are dormant, it is quite possible that excess malate dehydrogenase ensures restarting of the cycle for immediate energy production. Consequently, the concentration of excess malate dehydrogenase drops once the cycle is initiated and the production of NADH resumes. Thus, it also fits that there would be an increase of glucose-6-phoshate isomerase in germlings rather than uredospores because the germling needs to create pyruvate from glucose to enter the activated citric acid cycle. The observation that there are greater amounts of ADP:ATP translocases in the germlings points to the exchange of ADP for ATP in the mitochondria and keeping up with the amount of energy being expired.

Our results also agree with previously published studies on the biology of germinating uredospores from *Uromyces* spp. A uredopsore is suspended in the G2 phase of cell cycling, its doubling of DNA has occurred, and it is primed for mitosis (Kwon and Hoch 1991). Chromatin condensation coincides with nuclear migration as the germ tube elongates prior to appressorium formation (Kwon and Hoch 1991). Consequently, more histones need to be available for condensation and our finding of an increased amount of histone proteins in germlings rather than uredospores goes along with these prior observations.

Similarly, apical vesicles reorganize during germ tube elongation (Kwon et al. 1991a) and these apical vesicles contribute to apical growth (Grove and Bracker 1970). GTP-binding proteins have been linked to Golgi body-mediated secretory pathways and target vesicles to their cellular destinations (Kim et al. 2006). Our finding that GTP-binding proteins are abundant in germlings suggests that these proteins may be associated with the increased amounts of vesicle trafficking that occur during germination.

A well-organized cytoskeletal network also exists in elongating germlings (Hoch and Staples 1985). The actin and microtubule proteins likely contribute to a force that elongates the tube. This network follows the apical tip and the organization of these proteins is in constant flux until there is a clear differentiation toward the development of an appressorium (Kwon et al. 1991b); therefore, it is quite possible that the total concentration of actin and microtubules may not change, as supported by our data. The same could be said for the groups of translation elongation factors whose concentrations were very similar between germlings and uredospores. It is possible that the translation elongation factors harbored in the uredopore are used by the germling to quickly synthesize proteins not stored in the uredospore.

Septin, a protein involved in formation of the septum that seals off vacant cellular structures as the cytoplasm and nuclei migrate with the growing fungal apex, was not abundant in the germlings, possibly because appressoria had not formed. Rather, we detected septin in the uredospores. It is likely that the excess septin found in the uredospore was a remnant of the uredospore separating from uredial primordia (Muller et al. 1974).

Liberally viewed, our data also may allude to other protein accumulation changes that might be indicative of features important for pathogenicity, such as increased fatty acid or steroid synthesis needed for elongating membrane structures and an accumulation of chitinase needed to convert fungal cell wall carbohydrate composition from chitin to β-glucans (Freytag and Mendgen 1991a,b), a process that may help the fungus

avoid a salicylic acid signaling plant defense response that includes the accumulation of chitinases (Mellersh and Heath 2003).

We have used spectral count to estimate the relative abundance of a protein and measure a shift in protein accumulation during germination. However, other factors such as spectral variability and post-translational modification also could contribute to a change in spectral count. For example, spectral variability for an actin peptide could result in the assignment of spectra to a different actin record, giving the appearance of a shift in accumulation of one actin homolog over another. In this case, the evaluation of the accumulation of all matched actin proteins gives a more accurate picture of general actin accumulation changes but a less accurate determination for any one actin protein. Likewise, levels of a protein may appear to remain static between dormancy and germination but the protein becomes modified as a result of change in cellular state. Because biological post-translational modifications were not specifically accounted for, spectra reflecting such modifications might not have been matched and appropriately accounted for when determining the relative abundance as measured by spectral count. Consequently, specific protein accumulation changes that are recognized here will need to be verified using other independent methods.

Our study of the germling proteome was enhanced through comparative analysis with tandem mass spectra previously collected from the uredospore. It is interesting to point out that new proteins can be discovered from old spectral datasets when new information is added to the reference databases. This parallels searching old DNA sequence data against modern databases to gain a better understanding of genes whose identities were once unresolved. Here, the new sequences contributed to more than half of the identifications; clearly, the additional *U. appendiculatus* sequence data improved this dataset and the old one. It also should be noted that the *U. appendiculatu*s EST sequences were highly representative of the most abundant sequences that could be cloned, which ensured that we were most likely to detect the corresponding protein sequences. It follows, then, that the unknown proteins we identified also might be abundant. Thus, having the attributes of being abundant and unknown makes these proteins particularly interesting; they may be specific to and important for rust biology. Consequently, the rust cDNA sequences provide both a starting point for the discovery of novel proteins and serve as the next step toward gaining new insight on rusts. We expect that functional resolution of these unknown proteins and genes will provide additional details of the differences between actively growing germlings and quiescent uredospores.

MATERIALS AND METHODS

Plant inoculation.

Primary leaves of *Phaseolus vulgaris* cv. Pinto 111 were sprayed with a water suspension of *U. appendiculatus* race 41 uredospores (Pastor-Corrales 2003) containing 0.1% Tween 20 and 0.025% β-ionone (French et al. 1977). Spore density was adjusted such that there would be 2 to 4 pustules/cm^2 of leaf surface. Inoculated plants were placed in an 18°C dew chamber (Percival Scientific, Perry, IA, U.S.A.) overnight and the plants were grown at 23°C under fluorescent lighting.

cDNA Library construction.

Inoculated plant leaves were collected at 2, 4, 6, and 8 days postinoculation (dpi) and homogenized in a blender in 0.3 M sucrose, 0.1 M KH_2PO_4, and 3 mM $MgSO_4$ in a protocol adapted from Dekhuijzen and associates (1967). Essentially, the homogenate was filtered successively through 600-, 250-, 90-, and 45-μm sieves and the crude mycelia collected from the 45-μm mesh screen. Material that did not pass through the 600-, 250-, and 90-μm screens was collected and homogenized again at a higher blade speed and passed through the same series of sieves to increase the amount of mycelia collected from the 45-μm screen. These fractions contained fungal hyphae, haustoria, uredia, chloroplasts, and other plant debris such as xylem and broken cells (Fig. 1A and B). Further separation of the fractions through sucrose density gradients was not successful; however, chloroplast contamination was reduced with thorough washing on the 45-μm mesh screen. Septa and cytoplasmic streaming were observed in the purified hyphae, indicating that biological activity remained despite the intense processing. The same cytoplasmic streaming was not observed in other (broken) plant cells found in the fractions. RNA was purified from the material using a standard guanidinium isothiocyanate protocol (Koehler et al. 1996). To assess RNA purity, RT-PCR was used to compare the ratios of fungal RNA with plant RNA. Primers were designed to *P. vulgaris* and *U. appendiculatus* elongation factors 1-α and to the haustorium-specific Uf-RTP-1 gene (Hahn and Mendgen 1997; Kemen et al. 2005). These tests suggested that there was a clear enrichment of fungal RNA over plant RNA (Fig. 2). The Uf-RTP-1 gene marker was not readily present, indicating that haustoria were minor components of these fractions.

First- and second-strand cDNA was synthesized from 2 μg of mRNA using oligo d(T) primer with an *Not*I restriction site. *Eco*RI adaptors were ligated to both ends of the cDNAs and the cDNAs were directionally inserted into pBluescript (Invitrogen, Carlsbad, CA, U.S.A.). The library was normalized using previously described methods (Patanjali et al. 1991).

DNA sequencing.

Bacterial colonies were picked using a Genomic Solutions GenTAC-G3 colony picker (Ann Arbor, MI, U.S.A.) and placed into 384-well plates containing Luria broth with carbenicillin. Cultures were grown and transferred to 96-well plates. Plasmid DNA was extracted using a 96-well modified alkaline lysis protocol. DNA sequencing was performed using ABI BigDye Terminator (v3.1; Applied Biosystems, Foster City, CA, U.S.A.) according to the manufacturer's protocol, except that 5-μl reactions were performed with 0.25 μl of BigDye on an ABI 3730xl DNA sequencing machine with 50 cm arrays.

Electropherogram data was transferred from the ABI 3730xl sequencer computer to a Sun Solaris UltraSPARC II server. Phred was used to convert the electropherogram files to base and quality files (Ewing and Green 1998; Ewing et al. 1998). These files were examined by LUCY, which removed vector sequence and confirmed that each sequence was of high quality and read length (Chou and Holmes 2001). The LUCY output was transformed to FASTA format using a Perl script, Babalootoo (in-house modification of the TIGR Babaloo script). The sequences were assembled using the Genetics Computer Group software package (Accelrys, San Diego, CA, U.S.A.). To assure an efficient assembly of contiguous sequences, the Seqmerge assembly application was iterated three times using the same default settings for each assembly cycle. The consensus sequences then were exported and used in the BLAST searches described below to identify obvious plant sequences. The plant sequences were removed from the assembled set, the remaining contigs were disassembled to regenerate individual ESTs, and 11,325 sequences were submitted to NCBI GenBank dbEST.

Bioinformatics for identifying fungal DNA sequences.

The assembled DNA sequences and any remaining singletons were compared by BLAST on a Paracel server against

Arabidopsis thaliana cDNA and protein datasets, NCBI's nonredundant datasets (protein and nucleotide), the *Phakopsora pachyrhizi* trace dataset, the soybean EST dataset, the total EST dataset, and the GSS dataset, as well as TIGR's EST dataset for *Phaseolus vulgaris* and *P. coccineus*. This process was used to distinguish 81 plant DNA sequences. The remaining 2,226 sequences had either sufficient DNA or protein identity to known fungal sequences for *U. appendiculatus* and other Uredinales fungi or had no significant match to any plant or fungal organism represented in these databases.

Purification of proteins from germinating spores.

U. appendiculatus race 41 uredospores (50 mg) (Pastor-Corrales 2003) were resuspended in solution containing 100 mM mannitol, 3.3 mM KH_2PO_4, 1 mM $MgSO_4$, 0.033% Tween 20, and 0.025% β-ionone and adjusted to pH 6.5 with 2 M Na_2HPO_4. The β-ionone was used to induce germination for more than 90% of the spores (French et al. 1977) and the Tween 20 was used to help disperse and suspend the spores in solution. Mannitol was substituted for sucrose and the concentration was one-third of that previously used for sucrose (Dekhuijzen et al. 1967). In our preliminary tests, 100 mM mannitol was sufficient for eliminating cell lysis that occurred when germination was performed in hypotonic water (data not shown). The pH and the potassium concentrations were optimized to support the germination of submerged spores (Moloshok and Leinhos 1993). The mixed spore solutions were placed in an 18°C dew chamber for 5 h. The germlings (Fig. 1C) were collected by centrifugation and then pulverized with a mortar and pestle. Microscopy was used to confirm that the germ tubes had been disrupted by the grinding. Proteins released were precipitated in acetone and trichloroacetic acid, resolubilized in 8 M urea per 100 mM Tris HCl pH 8.5, reduced in trichloroethylphosphine, carboxyamidomethylated in iodoacetamide, and digested with endoproteinase Lys-C at 37°C for 12 h (Roche Applied Science, Indianapolis, IN, U.S.A.). The reaction then was diluted to 2 M urea with 100 mM Tris HCl pH 8.5, adjusted to 2 mM $CaCl_2$, and digested with Porozyme immobilized trypsin (Applied Biosystems, Foster City, CA, U.S.A.) at 37°C for 12 h as previously described (Florens and Washburn 2006). Immobilized trypsin was removed by centrifugation. All peptides were separated from spore and germling debris using 0.45 μm polyvinylidene diflouride filters (Millipore, Bedford, MA, U.S.A.) and were concentrated by solid-phase extraction using SPEC-PLUS PT C18 columns (Varian, Lake Forrest, CA, U.S.A.) followed by centrifugal vacuum evaporation.

Liquid chromatography separation of peptides.

Columns were prepared from 365 o.d. by 75 i.d. fused-silica capillaries (Polymicro Technologies, Phoenix, AZ, U.S.A.). Each capillary was drawn to a 5-μm tip using a P-2000 laser puller (Sutter Instrument Co., Novato, CA, U.S.A.) and packed under 600 psi of helium with 9 cm of 5-μm Aqua reverse phase C18 resin (Phenomenex, Torrance, CA, U.S.A.) followed by 4 cm of 5-μm Luna, a strong cation exchange resin (Phenomenex). The peptides were loaded onto the packed column using the same pressure cell at 600 psi. The loaded column then was placed in line with a Surveyor high-performance liquid chromatography pump that is part of the ProteomeX workstation (Thermo Electron, Waltham, MA, U.S.A.). Peptides were eluted as previously described in a 12-step process that included increasing concentrations of salt followed by an increasing gradient of mobile-phase at each step (Cooper et al. 2006). Flow rate was 200 nl/min. The eluent was electrosprayed directly into the electrospray ionization source of the LCQ-Deca XP ion trap mass spectrometer. Electrospray voltage (1.8 kV) was applied at a liquid junction before the column via a gold electrode.

Tandem mass spectrometry.

A parent ion scan was performed over the range 400 to 1,600 *m/z*. Automated peak recognition, dynamic exclusion, and tandem mass spectrometry (MS/MS) ion scanning of the top three most intense parent ions were performed using Xcalibur 1.3 (Thermo Electron). The tandem mass spectra were extracted from the raw data by Bioworks 3.2 (Thermo Electron). Parameters were set at 400 minimum mass, 3,500 maximum mass, 15 minimum peaks, 100,000 minimum total ion current, 1.4-Da precursor mass tolerance, 25 intermediate scans, and 1 group scan. All spectra not calculated as being singly charged were extracted as both doubly and triply charged spectra. A merge.pl script that is part of the Mascot 2.1 software package (Matrix Science, London) was used to convert multiple .dta files into a single file suitable for searching.

Peptide sequence inferences from spectra.

In all, 149,082 combined MS/MS spectra from four replicate experiments were evaluated by Mascot 2.1 (Matrix Science) (Perkins et al. 1999) and compared with virtual spectra created from peptides derived from a custom database. The database was composed of 355,242 protein records downloaded from NCBI on 13 July 2006 using the taxonomic search for "Fungi." In addition, 1,758 EST sequences were downloaded from NCBI on 13 July 2006 using the taxonomic search for "Uredinales" and were combined with 2,226 EST sequences generated from the *U. appendiculatus* cDNA sequencing project mentioned above. All EST sequences were searched against NCBI NR with BLASTX (Altschul et al. 1997). The reading frame from the best BLASTX alignment then was used to direct the translation of the EST. If there was no match, then the longest translatable open reading frame of all reading frames was appended and denoted as a "hypothetical translation." The derived protein sequences were appended to the custom database used for Mascot searching. Searches were performed on a seven-node 3.2-GHz Dell server. Search parameters were set at fully tryptic digests and one missed cleavage, carboxyamidomethylation was selected as a fixed mass modification, and oxidation (M) was set as a variable mass modification. Average mass values rather than monoisotopic mass values were used and peptide mass tolerance and fragment mass tolerance were set at ±1.5 and ±0.8 Da, respectively.

Assembly of proteins from peptides.

Mascot .dat files containing results from Mascot searches were uploaded to PANORAMICS, a web-based C program that assembles proteins from Mascot peptide assignments made to the collected tandem mass spectrometry data (Lee and Cooper 2006). PANORAMICS derives consistent probability-based confidence measures for protein assemblies which can be used to determine the false positive rate of identification (Feng et al. 2007). When computing the probability of a protein or group of proteins, the program takes into account both distinct peptides and shared peptides in a coherent manner by distributing the probabilities of shared peptides among all related proteins. The Mascot Ion Score, the database size, and the length and charge state of each peptide sequence are incorporated into the probability model. Proteins exceeding a 95% probability level were kept for evaluation. As a secondary test of the accuracy of the dataset, the germling tandem mass spectra were searched by Mascot against a version of the fungal database whereby all sequences were reversed and the data were processed by PANORAMICS. In all, 21 protein groups were assembled (95% level) and were deemed false matches

because none of the sequences that were matched existed in the forward sequence database (data not shown). This corresponds to a 4.6% false discovery rate, which agrees with the 95% confidence rate predicted by PANORAMICS for the described germling data.

PANORAMICS datasets containing peptide sequences, the number of tandem mass spectra associated with the same peptide sequence, the associated protein information, and the confidence indicators can be found in Supplementary Data 2.

Relative quantitation of protein amounts.

The amounts of proteins were estimated using a method similar to that of Zybailov and associates (2006). The numbers of tandem mass spectra identified for each peptide in a protein group were summed and divided by the molecular weight of the protein to normalize for the effects of finding different sets of peptides for a given protein. The counts for shared peptides were not divided by the number of other protein groups to which they also were associated because these peptides, although shared, were unlikely to be assigned to other protein groups exceeding the 95% threshold. In other words, the PANORAMICS probability model dictates that shared peptides in these groups contributed significantly to the identification of that group and should be counted equally with the distinct peptides. In the work of Zybailov and associates (2006), protein length was used as a normalizing factor, but molecular weight was used here and should be an equivalent because it is a product of protein length. The calculated value then was divided by the sum of spectral counts per molecular weight for all proteins exceeding the 95% threshold. The final value was the NSAF. The NSAFs for the germling protein groups were compared with the NSAFs for the same protein groups from the previously described uredospore dataset (Zybailov et al. 2006). Replicate datasets were combined, which eliminated the possibility of analyzing statistical deviation from run to run but preferentially maximized the number of peptides associated with each protein group, thus reducing the effects of deviation when quantifying by spectral count. It was demonstrated previously that reproducibility of spectral sampling grows along with the number of peptides associated with a protein and that fivefold differences in concentrations can be precisely evaluated (Liu et al. 2004). For our purposes, we accepted differences that rounded to 5.0.

LITERATURE CITED

Altschul, S. F., Madden, T. L., Schaffer, A. A., Zhang, J., Zhang, Z., Miller, W., and Lipman, D. J. 1997. Gapped BLAST and PSI-BLAST: A new generation of protein database search programs. Nucleic Acids Res. 25:3389-3402.

Beckmann, R. P., Mizzen, L. E., and Welch, W. J. 1990. Interaction of Hsp 70 with newly synthesized proteins: Implications for protein folding and assembly. Science 248:850-854.

Cargile, B. J., Bundy, J. L., and Stephenson, J. L., Jr. 2004. Potential for false positive identifications from large databases through tandem mass spectrometry. J. Proteome Res. 3:1082-1085.

Chou, H. H., and Holmes, M. H. 2001. DNA sequence quality trimming and vector removal. Bioinformatics 17:1093-1104.

Cooper, B., Garrett, W. M., and Campbell, K. B. 2006. Shotgun identification of proteins from uredospores of the bean rust *Uromyces appendiculatus*. Proteomics 6:2477-2484.

Dekhuijzen, H. M., Singh, H., and Staples, R. C. 1967. Some properties of hyphae isolated from bean leaves infected with the bean rust fungus. Contrib. Boyce Thompson Inst. 23:367-372.

Ewing, B., and Green, P. 1998. Base-calling of automated sequencer traces using phred. II. Error probabilities. Genome Res. 8:186-194.

Ewing, B., Hillier, L., Wendl, M. C., and Green, P. 1998. Base-calling of automated sequencer traces using phred. I. Accuracy assessment. Genome Res. 8:175-185.

Feng, J., Naiman, D. Q. and Cooper B. 2007. Probability model for assessing proteins assembled from peptide sequences inferred from tandem mass spectrometry data. Anal. Chem. 79(10):3901-3911

Florens, L., and Washburn, M. P. 2006. Proteomic analysis by multidimensional protein identification technology. Methods Mol. Biol. 328:159-175.

Florens, L., Washburn, M. P., Raine, J. D., Anthony, R. M., Grainger, M., Haynes, J. D., Moch, J. K., Muster, N., Sacci, J. B., Tabb, D. L., Witney, A. A., Wolters, D., Wu, Y., Gardner, M. J., Holder, A. A., Sinden, R. E., Yates, J. R., and Carucci, D. J. 2002. A proteomic view of the *Plasmodium falciparum* life cycle. Nature 419:520-526.

French, R. C., Graham, C. L., Gale, A. W., and Long, R. K. 1977. Structural and exposure time requirements for chemical stimulation of germination of uredospores of *Uromyces phaseoli*. Agric. Food Chem. 25:84-88.

Freytag, S., and Mendgen, K. 1991a. Surface carbohydrates and cell wall structure of in vitro-induced uredospore infection structures of *Uromyces viciae-fabae* before and after treatment with enzymes and alkali. Protoplasma 161:94-103.

Freytag, S., and Mendgen, K. 1991b. Carbohydrates on the surface of urediniospore- and basidiospore-derived infection structures of heteroecious and autoecious rust fungi. New Phytol. 119:527-534.

Frydman, J., Nimmesgern, E., Ohtsuka, K., and Hartl, F. U. 1994. Folding of nascent polypeptide chains in a high molecular mass assembly with molecular chaperones. Nature 370:111-117.

Grove, S. N., and Bracker, C. E. 1970. Protoplasmic organization of hyphal tips among fungi: Vesicles and Spitzenkorper. J. Bacteriol. 104:989-1009.

Hahn, M., and Mendgen, K. 1997. Characterization of in planta-induced rust genes isolated from a haustorium-specific cDNA library. Mol. Plant-Microbe Interact. 10:427-437.

Hall, N., Karras, M., Raine, J. D., Carlton, J. M., Kooij, T. W., Berriman, M., Florens, L., Janssen, C. S., Pain, A., Christophides, G. K., James, K., Rutherford, K., Harris, B., Harris, D., Churcher, C., Quail, M. A., Ormond, D., Doggett, J., Trueman, H. E., Mendoza, J., Bidwell, S. L., Rajandream, M. A., Carucci, D. J., Yates, J. R., 3rd, Kafatos, F. C., Janse, C. J., Barrell, B., Turner, C. M., Waters, A. P., and Sinden, R. E. 2005. A comprehensive survey of the *Plasmodium* life cycle by genomic, transcriptomic, and proteomic analyses. Science 307:82-86.

Heath, I. B., and Heath, M. C. 1976. Ultrastructure of mitosis in the cowpea rust fungus *Uromyces phaseoli* var. *vignae*. J. Cell Biol. 70:592-607.

Hoch, H. C., and Staples, R. C. 1985. The microtubule cytoskeleton in hyphae of *Uromyces phaseoli* germlings: Its relationship to the region of nucleation and to the F-actin cytoskeleton. Protoplasma 124:112-122.

Hoch, H., Staples, R., Whitehead, B., Comeau, J., and Wolf, E. 1987. Signaling for growth orientation and cell differentiation by surface topography in *Uromyces*. Science 235:1659-1662.

Kemen, E., Kemen, A. C., Rafiqi, M., Hempel, U., Mendgen, K., Hahn, M., and Voegele, R. T. 2005. Identification of a protein from rust fungi transferred from haustoria into infected plant cells. Mol. Plant-Microbe Interact. 18:1130-1139.

Kim, Y. G., Raunser, S., Munger, C., Wagner, J., Song, Y. L., Cygler, M., Walz, T., Oh, B. H., and Sacher, M. 2006. The architecture of the multisubunit TRAPP I complex suggests a model for vesicle tethering. Cell 127:817-830.

Koehler, S. M., Matters, G. L., Nath, P., Kemmerer, E. C., and Tucker, M. L. 1996. The gene promoter for a bean abscission cellulase is ethylene-induced in transgenic tomato and shows high sequence conservation with a soybean abscission cellulase. Plant Mol. Biol. 31:595-606.

Kwon, Y. H., and Hoch, H. C. 1991. Temporal and spatial dynamics of appressorium formation in *Uromyces appendiculatus*. Exp. Mycol. 15:116-131.

Kwon, Y. H., Hoch, H. C., and Aist, J. R. 1991a. Initiation of appressorium formation in *Uromyces appendiculatus*: Organization of the apex, and the responses involving microtubules and apical vesicles. Can. J. Bot. 69:2560-2573.

Kwon, Y. H., Hoch, H. C., and Staples, R. C. 1991b. Cytoskeletal organization in *Uromyces* urediospore germling apices during appressorium formation. Protoplasma 165:37-50.

Lee, J. J., and Cooper, B. 2006. Alternative workflows for plant proteomic analysis. Mol. BioSystems. 2:621-626.

Liu, H., Sadygov, R. G., and Yates, J. R., 3rd. 2004. A model for random sampling and estimation of relative protein abundance in shotgun proteomics. Anal. Chem. 76:4193-4201.

Lucier, G. L., and Jerardo, A. 2006. Vegetable and Melons Situation and Outlook Yearbook. E. R. S. Market and Trade Economics Division, United States Department of Agriculture, Washington, D.C.

Mellersh, D. G., and Heath, M. C. 2003. An investigation into the involvement of defense signaling pathways in components of the nonhost resistance of *Arabidopsis thaliana* to rust fungi also reveals a model system for studying rust fungal compatibility. Mol. Plant-Microbe Interact. 16:398-404.

Mendgen, K., Wirsel, S. G. R., Jux, A., Hoffmann, J., and Boland, W. 2006. Volatiles modulate the development of plant pathogenic rust fungi. Planta 224:1353-1361.

Moloshok, T. D., and Leinhos, G. M. E. 1993. The autogenic extracellular environment of *Uromyces appendiculatus* urediospore germlings. Mycologia 85:392-400.

Muller, L. V., Rijkenberg, F. H. T., and Truter, S. J. 1974. Ultrastructure of the uredial stage of *Uromyces appendiculatus*. Phytophylactica 6:73-104.

Nesvizhskii, A. I., and Aebersold, R. 2005. Interpretation of shotgun proteomic data: The protein inference problem. Mol. Cell Proteomics 4:1419-1440.

Pastor-Corrales, M. A. 2003. Sources, genes for resistance, and pedigrees of 52 rust and mosaic resistant dry bean germplasm lines released by the USDA Beltsville Bean Project in collaboration with the Michigan, Nebraska, and North Dakota Agricultural Experiment Station. Annu. Rep. Bean Improv. Coop. 46:235-240.

Pastor-Corrales, M. A., Miles, M. R., Hartman, G. L., and Frederick, R. D. 2006. Reaction of selected common bean cultivars to various isolates of *Phakopsora pachyrhizi*. In: 2006 Natl. Soybean Rust Symp. St. Louis.

Patanjali, S. R., Parimoo, S., and Weissman, S. M. 1991. Construction of a uniform-abundance (normalized) cDNA library. Proc. Natl. Acad. Sci. U.S.A. 88:1943-1947.

Perkins, D. N., Pappin, D. J., Creasy, D. M., and Cottrell, J. S. 1999. Probability-based protein identification by searching sequence databases using mass spectrometry data. Electrophoresis 20:3551-3567.

Schwartz, H. F. 1984. Dry bean management strategies in Colorado. Annu. Rep. Bean Improv. Coop. 27:6.

Smolka, M. B., Martins, D., Winck, F. V., Santoro, C. E., Castellari, R. R., Ferrari, F., Brum, I. J., Galembeck, E., Della Coletta Filho, H., Machado, M. A., Marangoni, S., and Novello, J. C. 2003. Proteome analysis of the plant pathogen *Xylella fastidiosa* reveals major cellular and extracellular proteins and a peculiar codon bias distribution. Proteomics 3:224-237.

Staples, R. C., and Hoch, H. C. 1988. Preinfection changes in germlings of a rust fungus induced by host contact. Pages 82-93 in: Biotechnology for Crop Protection. P. A. Hedin, J. J. Menn, and R. M. Hollingworth, eds. American Chemical Society, Washington, D.C.

Venette, J. R., and Jones, D. A. 1982. Yield losses associated with severity of bean rust (*Uromyces phaseoli*) on pinto beans (*Phaseolus vulgaris* UI-114). (Abstr.). Phytopathology 72:974.

Voegele, R. T., Struck, C., Hahn, M., and Mendgen, K. 2001. The role of haustoria in sugar supply during infection of broad bean by the rust fungus *Uromyces fabae*. Proc. Natl. Acad. Sci. U.S.A. 98:8133-8138.

Washburn, M. P., Wolters, D., and Yates, J. R., 3rd. 2001. Large-scale analysis of the yeast proteome by multidimensional protein identification technology. Nat. Biotechnol. 19:242-247.

Wegele, H., Muller, L., and Buchner, J. 2004. Hsp70 and Hsp90—a relay team for protein folding. Rev. Physiol. Biochem. Pharmacol. 151:1-44.

Yang, X., Dondeti, V., Dezube, R., Maynard, D. M., Geer, L. Y., Epstein, J., Chen, X., Markey, S. P., and Kowalak, J. A. 2004. DBParser: Web-based software for shotgun proteomic data analyses. J. Proteome Res. 3:1002-1008.

Zybailov, B., Coleman, M. K., Florens, L., and Washburn, M. P. 2005. Correlation of relative abundance ratios derived from peptide ion chromatograms and spectrum counting for quantitative proteomic analysis using stable isotope labeling. Anal. Chem. 77:6218-6224.

Zybailov, B., Mosley, A. L., Sardiu, M. E., Coleman, M. K., Florens, L., and Washburn, M. P. 2006. Statistical analysis of membrane proteome expression changes in *Saccharomyces cerevisiae*. J. Proteome Res. 5:2339-2347.